JOURNAL OF THE AMERICAN CHEMICAL SOCIETY

Communication

pubs.acs.org/JACS

Catalytic Four-Electron Reduction of O_2 via Rate-Determining Proton-Coupled Electron Transfer to a Dinuclear Cobalt-μ-1,2-peroxo Complex

Shunichi Fukuzumi,*[†,‡] Sukanta Mandal,[‡,§] Kentaro Mase,[†] Kei Ohkubo,[†] Hyejin Park,[‡] Jordi Benet-Buchholz,[§] Wonwoo Nam,*[‡] and Antoni Llobet*[‡,§]

[†]Department of Material and Life Science, Graduate School of Engineering, Osaka University, and ALCA, Japan Science and Technology Agency, Suita, Osaka 565-0871, Japan

[‡]Department of Bioinspired Science, Ewha Womans University, Seoul 120-750, Korea

[§]Institute of Chemical Research of Catalonia, Avinguda Països Catalans 16, E-43007 Tarragona, Spain

Supporting Information

ABSTRACT: Four-electron reduction of O_2 by octamethylferrocene (Me_8Fc) occurs efficiently with a dinuclear cobalt-μ-1,2-peroxo complex, **1**, in the presence of trifluoroacetic acid in acetonitrile. Kinetic investigations of the overall catalytic reaction and each step in the catalytic cycle showed that proton-coupled electron transfer from Me_8Fc to **1** is the rate-determining step in the catalytic cycle.

The catalytic four-electron ($4e^-$) reduction of O_2 to water has merited increasing attention because it is intrinsic to respiration[1] as well as fuel cell technology.[2] In fuel cells, the $4e^-$ reduction of O_2 is catalyzed at the cathode by Pt impregnated in carbon.[2,3] The high loadings of this precious metal that are required to achieve appreciable activity have prompted the development of catalysts based on nonprecious metals such as Co, Cu, and Fe.[4−7] In addition to electrocatalytic reduction of O_2 with nonprecious metal complexes, homogeneous catalytic reduction of O_2 by one-electron ($1e^-$) reductants such as ferrocene (Fc) derivatives has provided mechanistic insight into the key question: How can the two-electron ($2e^-$) versus $4e^-$ reduction of O_2 be controlled by metal complexes?[8−13] The key intermediate for the catalytic $4e^-$ reduction of O_2 is usually regarded to be a dinuclear metal−peroxo complex, which is further reduced to water. However, there has been no study of the electron-transfer (ET) reduction of isolated dinuclear metal−peroxo complexes with structures established by X-ray crystallography. Thus, the exact role of the dinuclear complex in the catalytic $4e^-$ reduction of O_2 has yet to be uncovered.

We report that a dinuclear cobalt-μ-1,2-peroxo complex with bis(pyridyl)pyrazolate (bpp) and terpyridine (trpy) ligands, $[Co^{III}_2(trpy)_2(\mu\text{-bpp})(\mu\text{-}1,2\text{-}O_2)]^{3+}$ (**1**), catalyzes the $4e^-$ reduction of O_2 by Fc derivatives in the presence of trifluoroacetic acid (TFA) in MeCN at 298 K. The structure of **1** was successfully determined by X-ray crystallography. Kinetic studies of the overall catalytic cycle and each step in the catalytic cycle enabled us to show for the first time that proton-coupled electron transfer (PCET) reduction of **1** is the rate-determining step in the overall catalytic $4e^-$ reduction of O_2.

Complex **1** was synthesized by the reaction of $Co(trpy)Cl_2$ with bpp under O_2 in methanol [Figure 1; also see the Experimental Section in the Supporting Information (SI)]. The aqua−hydroxo complex **2** was obtained by oxidation of $[Co^{II}_2(trpy)_2(\mu\text{-bpp})(\mu\text{-Cl})](PF_6)_2$ with cerium(IV) ammonium nitrate (Figure 1; also see the SI). Both **1** and **2** were well-characterized by spectroscopic methods (Figures S3−S6 in the SI) and X-ray crystallography (Figure 2). The X-ray structure of **1** (Figure 2a) shows that the peroxo ligand is coordinated to the two Co^{III} ions in a μ-1,2 fashion. The O−O bond distance, 1.397(2) Å, is typical for dinuclear Co−peroxo complexes.[14] The structure of **2** (Figure 2b) shows that the aqua and hydroxo ligands are coordinated to the two Co^{III} ions and share a H atom. The O−O distance of 2.415 Å is long enough to accommodate the H atom.

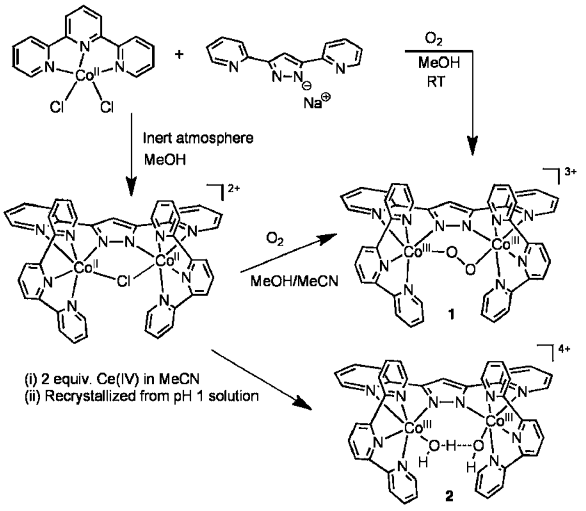

Figure 1. Syntheses of complexes **1** and **2**.

The $4e^-$ reduction of O_2 by octamethylferrocene (Me_8Fc) occurred with a catalytic amount of **1** in the presence of TFA in MeCN at 298 K (Figure 3a), with complete conversion of

Received: April 17, 2012
Published: June 1, 2012

dx.doi.org/10.1021/ja303674n | *J. Am. Chem. Soc.* 2012, 134, 9906−9909

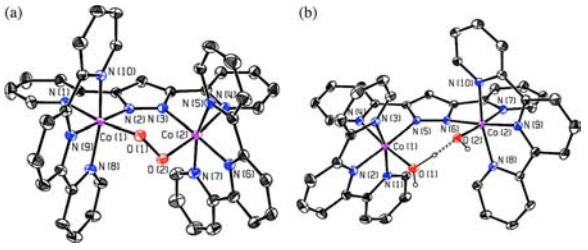

Figure 2. ORTEP plots (50% probability) of the crystal structures of the cationic parts of (a) **1** and (b) **2**. H atoms, counteranions, and solvent molecules of crystallization have been omitted for clarity.

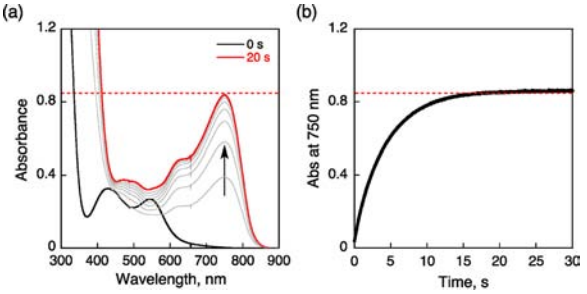

Figure 3. (a) Absorption spectral changes in the 4e$^-$ reduction of O_2 by Me_8Fc (2 mM) catalyzed by **1** (25 μM) in the presence of TFA (50 mM) in O_2-saturated MeCN at 298 K. The black and red lines show the spectra before and after addition of TFA, respectively. The dotted line is the absorbance at 750 nm due to 2 mM Me_8Fc^+. (b) Time profile of the absorbance at 750 nm due to Me_8Fc^+.

Me_8Fc to Me_8Fc^+ (λ_{max} = 750 nm, ε = 410 M^{-1} cm^{-1}). Iodometric titrations confirmed that no H_2O_2 was formed after the reaction was complete (Figure S7). Thus, **1** catalyzes the 4e$^-$ reduction of O_2 by Me_8Fc in the presence of TFA in MeCN:

$$4Me_8Fc + O_2 + 4H^+ \xrightarrow{\mathbf{1}} 4Me_8Fc^+ + H_2O \qquad (1)$$

The time profile in Figure 3b indicates that this process proceeds in a single step rather than by stepwise reduction of O_2 to H_2O_2 and then to H_2O. When **1** was replaced by **2**, the 4e$^-$ reduction of O_2 by Me_8Fc occurred at the same rate (Figure S8).

The formation of Me_8Fc^+ obeyed pseudo-first-order kinetics (Figure 3b). The pseudo-first-order rate constant (k_{obs}) increased linearly with increasing concentration of **1** (Figure 4a) but did not depend on the O_2 concentration (Figure 4b). Thus, the kinetic equation is

$$\frac{d[Me_8Fc^+]}{dt} = k_{cat}[Me_8Fc][\mathbf{1}] \qquad (2)$$

where k_{cat} is the second-order rate constant for the catalytic 4e$^-$ reduction of O_2 by Me_8Fc. k_{cat} increased with increasing TFA concentration with a nonzero intercept (Figure 5a). The 4e$^-$ reduction of O_2 by decamethylferrocene (Fc*) catalyzed by **1** in the presence of TFA in MeCN at 298 K occurred more efficiently than that by Me_8Fc (Figure S9).[15]

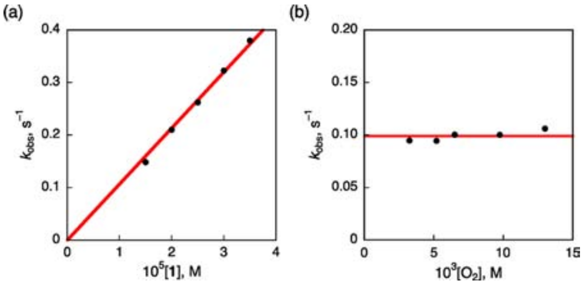

Figure 4. Plots of (a) k_{obs} vs [**1**] in O_2-saturated MeCN and (b) k_{obs} vs [O_2] with [**1**] = 25 μM for the 4e$^-$ reduction of O_2 by Me_8Fc (1.5 mM) in the presence of TFA (50 mM) in MeCN.

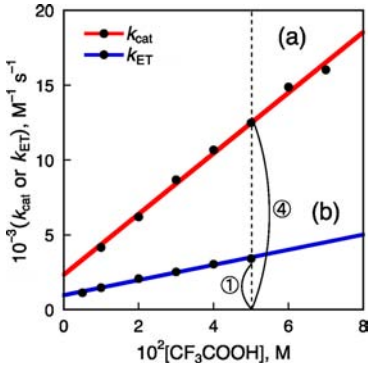

Figure 5. (a) Plot of k_{cat} vs TFA concentration for the catalytic 4e$^-$ reduction of O_2 by Me_8Fc (1.5 mM) in O_2-saturated MeCN at 298 K. (b) Plot of k_{ET} vs TFA concentration for the reaction involving ET from Me_8Fc (1.5 mM) to **1** (25 μM) in deaerated MeCN at 298 K.

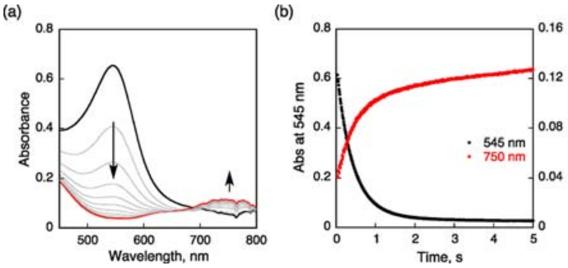

Figure 6. (a) Absorption spectral changes in the reduction of **1** (50 μM) by Me_8Fc (1.5 mM) in the presence of TFA (50 mM) in deaerated MeCN. (b) Time profiles of the absorbance at 545 nm due to decreasing **1** (black) and 750 nm due to increasing Me_8Fc^+ (red).

The 4e$^-$ reduction of O_2 requires the reduction of **1** by Me_8Fc. Thus, we examined the reduction of **1** by Me_8Fc in the absence and presence of TFA in deaerated MeCN. In the absence of TFA, no reduction of **1** by Me_8Fc was observed. In the presence of TFA, however, **1** was efficiently reduced by Me_8Fc (Figure 6a), as the absorption band at 545 nm due to **1** disappeared, accompanied by the appearance of the absorption band at 750 nm due to Me_8Fc^+. The decay rate of **1** coincided with the rate of formation of Me_8Fc^+ (Figure 6b). The stoichiometry of the PCET reduction of **1** by Me_8Fc was determined to be

$$\begin{aligned} &4Me_8Fc + [Co^{III}(O_2)Co^{III}]^{3+} + 4H^+ \\ &\quad \rightarrow 4Me_8Fc^+ + [Co^{II}{-}Co^{II}]^{3+} + 2H_2O \end{aligned} \qquad (3)$$

The ET from Me_8Fc to **1** in the presence of TFA obeyed pseudo-first-order kinetics (Figure S10a), and k_{obs} increased linearly with increasing [Me_8Fc] concentration (Figure S10b). Thus, the decay rate of **1** is given by

$$-\frac{d[\mathbf{1}]}{dt} = \frac{1}{4}\frac{d[Me_8Fc^+]}{dt} = k_{ET}[\mathbf{1}][Me_8Fc] \qquad (4)$$

where k_{ET} is the second-order rate constant for ET from Me_8Fc to **1** in the presence of TFA. Because 4 equiv of Me_8Fc^+ are produced by ET from Me_8Fc to **1** in the presence of TFA, the decay rate of **1** is equal to one-fourth the formation rate of Me_8Fc^+ (eq 4). The k_{ET} value increased linearly with increasing TFA concentration with a nonzero intercept (Figure 5b). The intercept corresponds to ET from Me_8Fc to **1**, which is followed by much faster PCET, and the linear dependence of k_{ET} on [TFA] suggests that initial ET from Me_8Fc to **1** is accelerated by the acid. Although no protonation of **1** by TFA was observed, as indicated by the absence of absorption spectral changes for **1** in the presence of TFA (Figure S11a), absorption spectral changes due to demetalation of **1** were observed in the presence of $HClO_4$, which is a much stronger acid than TFA (Figure S11b). Since k_{ET} increased linearly with increasing TFA concentration (Figure 5b), ET from Me_8Fc to protonated **1**, whose concentration is proportional to the TFA concentration, may be much faster than ET from Me_8Fc to **1**.

Comparison of k_{cat} and k_{ET} at various TFA concentrations (Figure 5) showed k_{cat} always to be 4 times as large as k_{ET}. This indicates that the PCET reduction of **1** by Me_8Fc is the rate-determining step in the overall catalytic cycle of the 4e$^-$ reduction of O_2 by Me_8Fc in the presence of TFA in MeCN.

The k_{ET} values for ET from Fc* to **1** in the presence of TFA in MeCN were also determined at 298 K and found to be ~10 times larger than those for Me_8Fc, as expected given the lower 1e$^-$ oxidation potential of Fc* (E_{ox} = −0.08 V vs SCE) than of Me_8Fc (E_{ox} = −0.04 V vs SCE).[9]

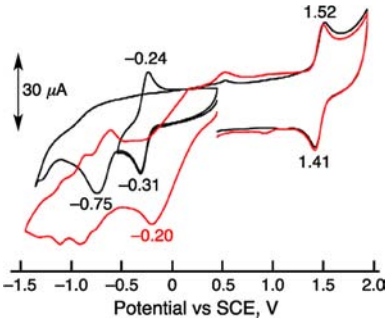

Figure 7. CVs of **1** in MeCN (1 mM) without TFA in the presence of 0.10 M $TBAPF_6$ (black) and with 2 mM TFA (red). Sweep rate = 100 mV s^{-1}.

To confirm the thermodynamics of PCET from Me_8Fc to **1**, cyclic voltammograms (CVs) of **1** were measured in the absence and presence of TFA in MeCN (Figure 7). In the absence of TFA, the reversible Co^{III}_2/$Co^{III}Co^{II}$ and $Co^{IV}Co^{III}$/Co^{III}_2 couples were observed at $E_{1/2}$ = −0.27 and +1.47 V vs SCE, respectively. The cathodic peak current observed at −0.75 V corresponds to the reduction of $Co^{III}Co^{II}$ to Co^{II}_2. However, this reduction was irreversible, probably because of the O−O bond cleavage in the dissociative ET reduction. In the presence of TFA, the reversible $Co^{IV}Co^{III}$/Co^{III}_2 couple remained the same as that in the absence of TFA, whereas the Co^{III}_2/$Co^{III}Co^{II}$ reduction peak was shifted in the positive direction.[16] This is consistent with the previous results for ET from Me_8Fc to **1**, as ET from Me_8Fc (E_{ox} = −0.04 V vs SCE) to **1** (E_{red} = −0.27 V vs SCE) is thermodynamically unfavorable but becomes energetically feasible in the presence of TFA.

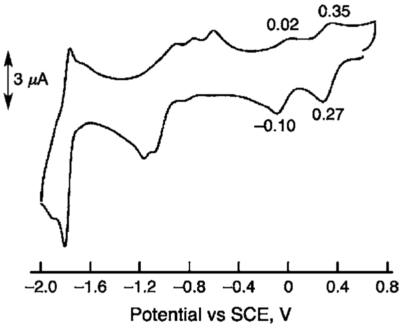

Figure 8. CV of **2** in MeCN (0.25 mM) in the presence of 0.10 M $TBAPF_6$. Sweep rate = 100 mV s^{-1}.

Figure 8 shows a CV for aqua−hydroxo complex **2**. The two reversible couples observed at +0.31 and −0.04 V vs SCE correspond to the first 1e$^-$ reduction of **2** to the $Co^{III}Co^{II}$ complex and the second 1e$^-$ reduction to the Co^{II}_2 complex, respectively. On the basis of the E_{red} values for **2**, ET from Me_8Fc to **2** to produce 2 equiv of Me_8Fc^+ and the Co^{II}_2 complex is thermodynamically feasible. In fact, ET from Me_8Fc to **2** occurs in two steps with rate constants of 3.2 × 10^5 and 1.6 × 10^3 M^{-1} s^{-1} for the first and second steps, respectively (Figures S12 and S13).

When **2** was reduced by 2 equiv of Me_8Fc, the peroxo complex was produced by the reaction of the reduced **2** with O_2 (Figure 9a), as the absorption band due to **1** (λ_{max} = 545 nm) appeared together with that of Me_8Fc^+ (λ_{max} = 750 nm). The rate of formation of **1** increased with increasing TFA concentration (Figure 9b). Because the formation of **1** is much faster than the PCET reduction of **1**,[17] the formation of **1** in the catalytic cycle is not the rate-determining step.

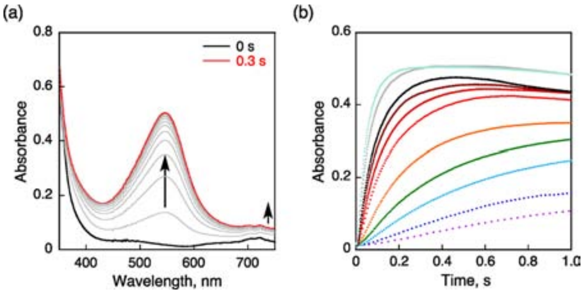

Figure 9. (a) Transient absorption spectral changes in the reaction of **2** (50 μM) with Me_8Fc (100 μM) in the presence of TFA (30 mM) in air-saturated MeCN. (b) Time profiles of the absorbance at 545 nm due to **1** in the reaction of **2** with Me_8Fc in the presence of various concentrations of TFA (100 μM to 30 mM) in air-saturated MeCN.

The overall catalytic cycle is summarized in Scheme 1. When the reaction is started from peroxo complex **1**, **1** is reduced by PCET from Me_8Fc. Because the decay rate of **1** coincides with the rate of formation of 4 equiv of Me_8Fc^+, once **1** is reduced by PCET, the subsequent PCET processes should be much faster

Scheme 1

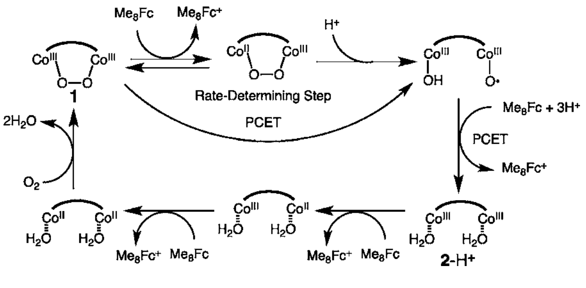

than the initial PCET process. The reduction of **1** by Me_8Fc can proceed via two pathways. One involves ET from Me_8Fc to **1** followed by protonation of the reduced **1**, which results in O−O bond cleavage. This is followed by rapid PCET to produce **2**. The other pathway involves coupling of the ET and the protonation, which occur in a concerted manner, since the PCET rate constant increases linearly with increasing TFA concentration (Figure 5). After **1** is converted to **2**, a fast ET reduction of **2** by Me_8Fc occurs, producing the Co^{II}_2 complex, which reacts with O_2 to regenerate **2**. When the reaction is started from **2**, **2** is converted rapidly to **1** by ET reduction of **2** and the reaction of the Co^{II} complex with O_2, both of which are much faster than the PCET reduction of **1**. Thus, the same catalytic rate is observed starting from **1** or **2**. Because the rate of formation of **1** from **2** with Me_8Fc increases with increasing TFA concentration (Figure 9), this process may also proceed via a PCET pathway, although the detailed mechanism has yet to be clarified.[18]

In conclusion, the $4e^-$ reduction of O_2 by Me_8Fc in the presence of TFA is efficiently catalyzed by the dinuclear Co^{III}−peroxo complex **1** as well as the aqua−hydroxo complex **2**. The X-ray structures of both **1** and **2** were successfully determined. Kinetic analyses of the overall catalytic process and each catalytic step revealed that PCET reduction of **1** is the rate-determining step in the overall catalytic cycle, which may not be the same as the natural process in respiration, however.

■ ASSOCIATED CONTENT

Ⓢ Supporting Information

Experimental section, additional data, and complete ref 3. This material is available free of charge via the Internet at http://pubs.acs.org.

■ AUTHOR INFORMATION

Corresponding Author

fukuzumi@chem.eng.osaka-u.ac.jp; wwnam@ewha.ac.kr; allobet@ICIQ.ES

Notes

The authors declare no competing financial interest.

■ ACKNOWLEDGMENTS

This work was supported in part by Grants-in-Aid (20108010 to S.F. and 23750014 to K.O.) and a Global COE Program (to S.F.) from MEXT of Japan, by NRF/MEST of Korea through WCU Project R31-2008-000-10010-0 (to W.N.), and by MICINN of Spain (CTQ2010-21497 to A.L.).

■ REFERENCES

(1) (a) Ferguson-Miller, S.; Babcock, G. T. *Chem. Rev.* **1996**, *96*, 2889. (b) Babcock, G. T.; Wikström, M. *Nature* **1992**, *356*, 301. (c) Babcock, G. T. *Proc. Natl. Acad. Sci. U.S.A.* **1999**, *96*, 12971. (d) Kaila, V. R. I.; Verkhovsky, M. I.; Wikström, M. *Chem. Rev.* **2010**, *110*, 7062.

(2) (a) Stambouli, A. B.; Traversa, E. *Renewable Sustainable Energy Rev.* **2002**, *6*, 295. (b) Marković, N. M.; Schmidt, T. J.; Stamenković, V.; Ross, P. N. *Fuel Cells* **2001**, *1*, 105. (c) Steele, B. C. H.; Heinzel, A. *Nature* **2001**, *414*, 345.

(3) Borup, R.; et al. *Chem. Rev.* **2007**, *107*, 3904.

(4) (a) Lee, K.; Zhang, L.; Zhang, J. In *PEM Fuel Cell Electrocatalysts and Catalyst Layers*; Springer: London, 2008; p 715. (b) Anson, F. C.; Shi, C.; Steiger, B. *Acc. Chem. Res.* **1997**, *30*, 437. (c) Wang, B. *J. Power Sources* **2005**, 152. (d) Peljo, P.; Rauhala, T.; Murtomäki, L.; Kallio, T.; Kontturi, K. *Int. J. Hydrogen Energy* **2011**, *36*, 10033.

(5) (a) Collman, J. P.; Devaraj, N. K.; Decréau, R. A.; Yang, Y.; Yan, Y.-L.; Ebina, W.; Eberspacher, T. A.; Chidsey, C. E. D. *Science* **2007**, *315*, 1565. (b) Collman, J. P.; Decréau, R. A.; Lin, H.; Hosseini, A.; Yang, Y.; Dey, A.; Eberspacher, T. A. *Proc. Natl. Acad. Sci. U.S.A.* **2009**, *106*, 7320. (c) Collman, J. P.; Ghosh, S.; Dey, A.; Decréau, R. A.; Yang, Y. *J. Am. Chem. Soc.* **2009**, *131*, 5034.

(6) (a) Kadish, K. M.; Frémond, L.; Shen, J.; Chen, P.; Ohkubo, K.; Fukuzumi, S.; El Ojaimi, M.; Gros, C. P.; Barbe, J.-M.; Guilard, R. *Inorg. Chem.* **2009**, *48*, 2571. (b) Kadish, K. M.; Shen, J.; Frémond, L.; Chen, P.; Ojaimi, M. E.; Chkounda, M.; Gros, C. P.; Barbe, J.-M.; Ohkubo, K.; Fukuzumi, S.; Guilard, R. *Inorg. Chem.* **2008**, *47*, 6726. (c) Chen, W.; Akhigbe, J.; Brückner, C.; Li, C. M.; Lei, Y. *J. Phys. Chem. C* **2010**, *114*, 8633.

(7) (a) Rosenthal, J.; Nocera, D. G. *Acc. Chem. Res.* **2007**, *40*, 543. (b) Dogutan, D. K.; Stoian, S. A.; McGuire, R.; Schwalbe, M.; Teets, T. S.; Nocera, D. G. *J. Am. Chem. Soc.* **2011**, *133*, 131. (c) Teets, T. S.; Cook, T. R.; McCarthy, B. D.; Nocera, D. G. *J. Am. Chem. Soc.* **2011**, *133*, 8114.

(8) (a) Fukuzumi, S. *Prog. Inorg. Chem.* **2009**, *56*, 49. (b) Fukuzumi, S. *Bull. Chem. Soc. Jpn.* **1997**, *70*, 1. (c) Fukuzumi, S.; Ohkubo, K. *Coord. Chem. Rev.* **2010**, *254*, 372. (d) Fukuzumi, S. *Chem. Lett.* **2008**, *37*, 808.

(9) (a) Fukuzumi, S.; Mochizuki, S.; Tanaka, T. *Inorg. Chem.* **1989**, *28*, 2459. (b) Fukuzumi, S.; Mochizuki, S.; Tanaka, T. *Inorg. Chem.* **1990**, *29*, 653. (c) Fukuzumi, S.; Mochizuki, S.; Tanaka, T. *J. Chem. Soc., Chem. Commun.* **1989**, 391.

(10) (a) Fukuzumi, S.; Okamoto, K.; Gros, C. P.; Guilard, R. *J. Am. Chem. Soc.* **2004**, *126*, 10441. (b) Fukuzumi, S.; Okamoto, K.; Tokuda, Y.; Gros, C. P.; Guilard, R. *J. Am. Chem. Soc.* **2004**, *126*, 17059.

(11) Halime, Z.; Kotani, H.; Li, Y.; Fukuzumi, S.; Karlin, K. D. *Proc. Natl. Acad. Sci. U.S.A.* **2011**, *108*, 13990.

(12) (a) Peljo, P.; Murtomäki, L.; Kallio, T.; Xu, H.-J.; Meyer, M.; Gros, C. P.; Barbe, J.-M.; Girault, H. H.; Laasonen, K.; Kontturi, K. *J. Am. Chem. Soc.* **2012**, *134*, 5974. (b) Su, B.; Hatay, I.; Trojánek, A.; Samec, Z.; Khoury, T.; Gros, C. P.; Barbe, J.-M.; Daina, A.; Carrupt, P.-A.; Girault, H. H. *J. Am. Chem. Soc.* **2010**, *132*, 2655. (c) Hatay, I.; Su, B.; Li, F.; Méndez, M. A.; Khoury, T.; Gros, C. P.; Barbe, J.-M.; Ersoz, M.; Samec, Z.; Girault, H. H. *J. Am. Chem. Soc.* **2009**, *131*, 13453.

(13) (a) Devoille, A. M. J.; Love, J. B. *Dalton Trans.* **2012**, *41*, 65. (b) Askarizadeh, E.; Yaghoob, S. B.; Boghaei, D. M.; Slawin, A. M. Z.; Love, J. B. *Chem. Commun.* **2010**, *46*, 710.

(14) (a) Givaja, G.; Volpe, M.; Edwards, M. A.; Blake, A. J.; Wilson, C.; Schröder, M.; Love, J. B. *Angew. Chem., Int. Ed.* **2007**, *46*, 584. (b) Volpe, M.; Hartnett, H.; Leeland, J. W.; Wills, K.; Ogunshun, M.; Duncombe, B. J.; Wilson, C.; Blake, A. J.; McMaster, J.; Love, J. B. *Inorg. Chem.* **2009**, *48*, 5195.

(15) When Me_8Fc was replaced by 1,1′-dimethylferrocene (Me_2Fc), which is a weaker electron donor, no catalytic $4e^-$ reduction of O_2 occurred in the presence of TFA in MeCN because the ET reduction of **1** by Me_2Fc is thermodynamically unfavorable.

(16) Although detailed analysis of the CV at negative potentials (ca. −1 V) has yet to be performed, these peaks may correspond to the $1e^-$ and $2e^-$ reduction processes of Co^{II}_2 complex **2**, which were observed in the CV of **2** (Figure 8), as the ET reduction of **1** in the presence of TFA results in O−O bond cleavage (eq 3).

(17) The rate constant for the formation of **1** from **2** with Me_8Fc at [TFA] = 30 mM (Figure 9b) was 1.8×10^5 M^{-1} s^{-1}, which is much larger than k_{ET} for the PCET reduction of **1** by Me_8Fc at the same TFA concentration (2.5×10^3 M^{-1} s^{-1}; Figure 5).

(18) The rate constant of 1.8×10^5 M^{-1} s^{-1} for the formation of **1** from **2** with Me_8Fc at [TFA] = 30 mM is much larger than that for the second-step ET from Me_8Fc to the $Co^{III}Co^{II}$ complex (1.6×10^3 M^{-1} s^{-1}; Figure S13). Thus, the $Co^{III}Co^{II}$ complex produced by the first-step ET from M_8Fc to **2** may react with O_2 by a PCET process prior to the second-step ET from Me_8Fc to the $Co^{III}Co^{II}$ complex.